

Disproportional surface segregation in ligand-free gold-silver alloy solid solution nanoparticles and its implication for catalysis and biomedicine

Frederic Stein ^a, Sebastian Kohsakowski ^b, Ricardo Martinez Hincapie ^c, Christoph Rehbock ^a, Sven Reichenberger ^a, Viktor Colic ^c, Daniel Guay ^d, Stephan Barcikowski ^{a*}

a. Technical Chemistry I, Center for Nanointegration Duisburg-Essen (CENIDE), University of Duisburg Essen, D-45141 Essen, Germany.

b. Laufenberg GmbH, D-47839 Krefeld, Germany.

c. Max Planck Institute for Chemical Energy Conversion, D-45470 Mülheim an der Ruhr, Germany.

d. Institut National de la Recherche Scientifique, INRS-Énergie, Matériaux et Télécommunications, Varennes, Québec J3X 1S2, Canada.

Supporting Information

Nanoparticle characterization

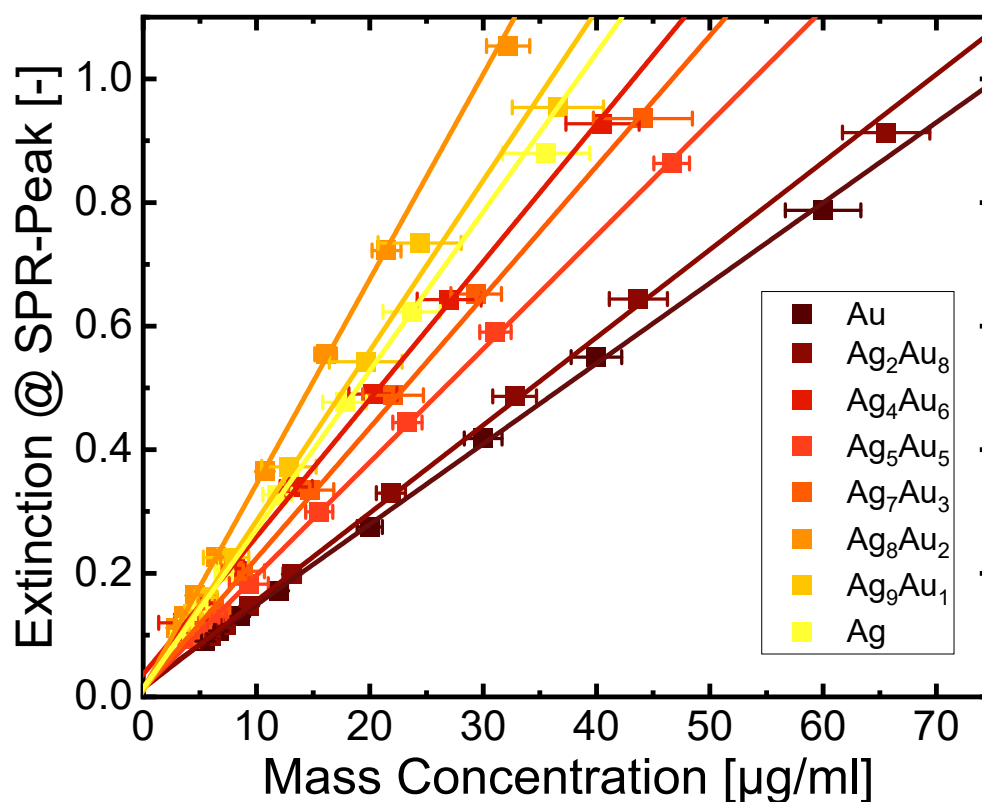


Figure S1 - Extinction values at the SPR peaks of the corresponding compositions measured at various known mass concentrations. The linear fits for every dataset allow the calculation of the mass concentration of a colloid with unknown composition. The error bars are standard deviations from triplicates.

Figure S1 shows the constructed calibration lines used to calculate the mass concentrations of all colloids used in this study. Colloids with known mass concentrations were diluted to various concentrations and UV/Vis spectra were collected to construct these calibration lines. From these spectra, the distinct extinction value of the SPR peak was extrapolated. Afterward, linear fits were applied for each composition, which allowed to calculate the mass-concentration of every colloid as long as the composition is known following:

$$\text{mass concentration} = a + b \cdot \text{extinction @ SPR peak} \quad (1)$$

Here, a is the intercept, and b is the slope of the fit. For all slope and intercept values, see Table S1.

Table S1 - Intercept and slope of each used composition in this study. All values are extrapolated from the linear fits in Figure S2.

Composition	Intercept [-]	Slope [ml/μg]
Au	-1.47	76.86
Ag ₂₀ Au ₈₀	-0.94	70.15
Ag ₄₀ Au ₆₀	-1.13	43.95
Ag ₅₀ Au ₅₀	-0.90	54.84
Ag ₇₀ Au ₃₀	-0.51	46.44
Ag ₈₀ Au ₂₀	-0.50	30.94
Ag ₉₀ Au ₁₀	-0.51	36.92
Ag	-0.57	39.15

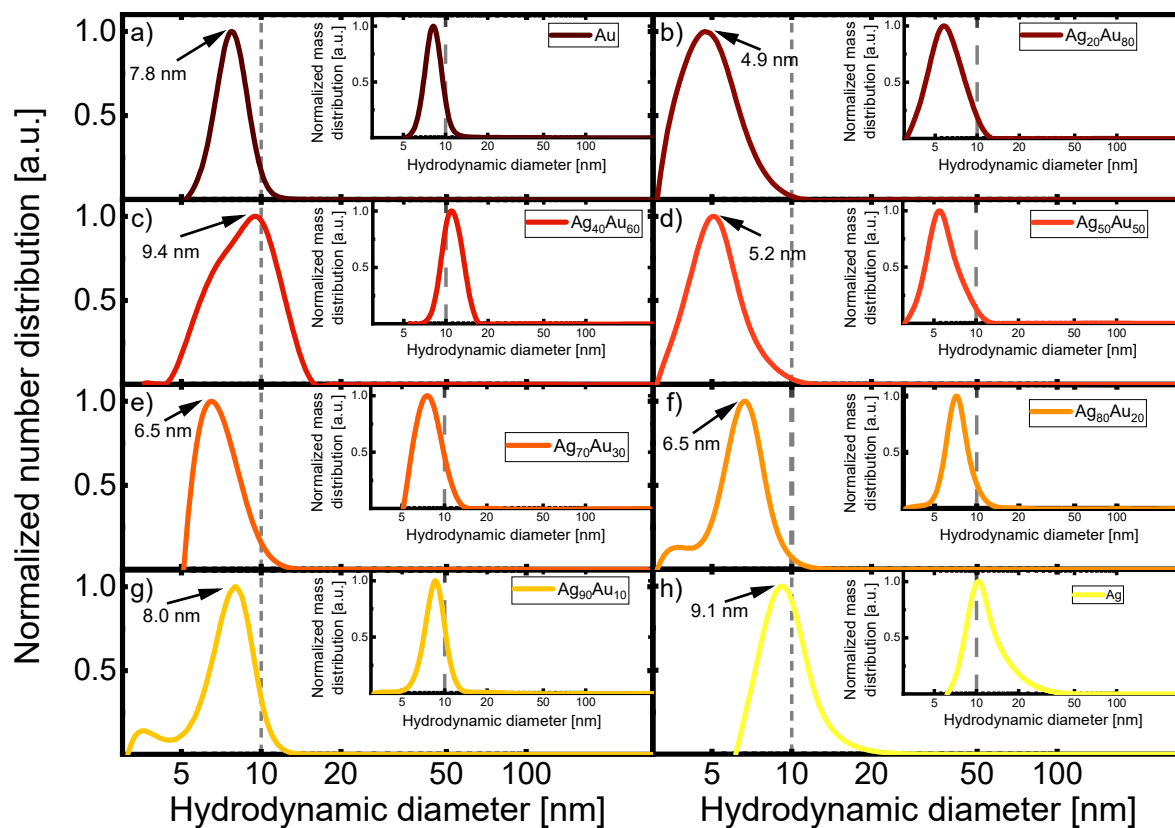


Figure S2 - Number-weighted hydrodynamic size distributions of the colloidal (a) pure gold NP, alloy NP with intermediate compositions as indicated in the legend (b-g), and pure silver NP (h) derived from ADC measurements. The inserts show the respective mass-weighted distributions. All distributions are normalized to their peak diameter for better comparability.

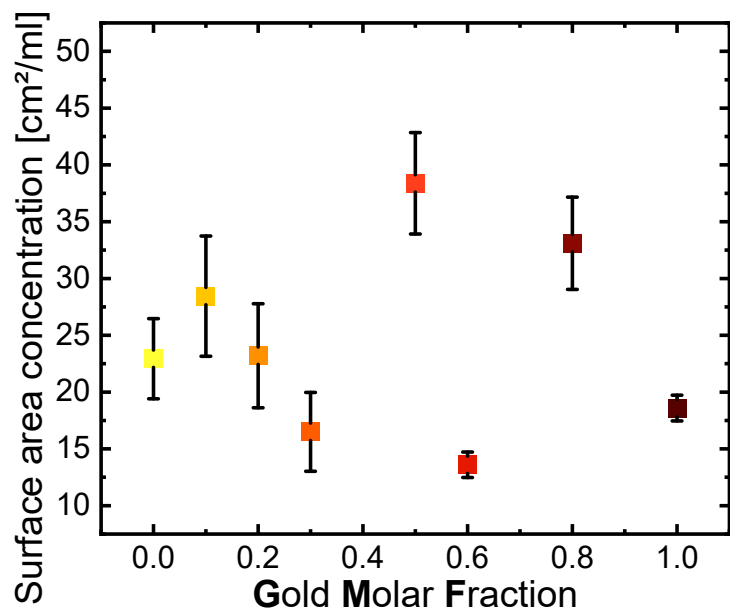
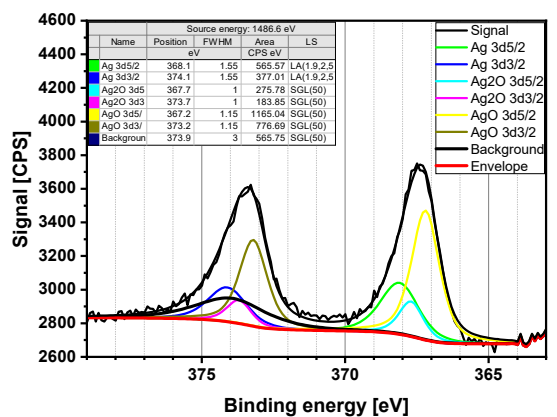
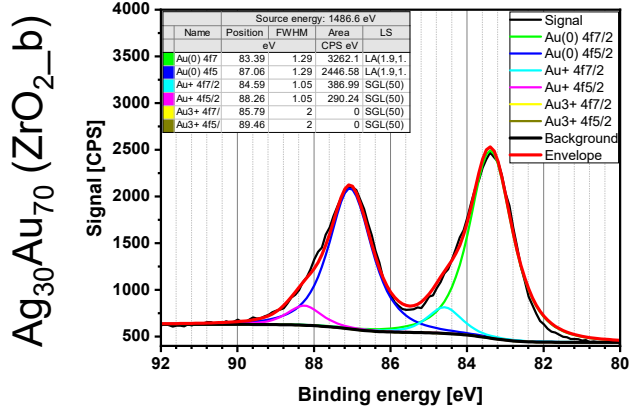
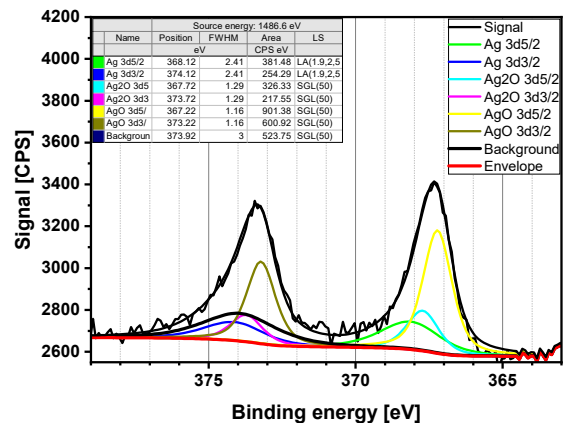
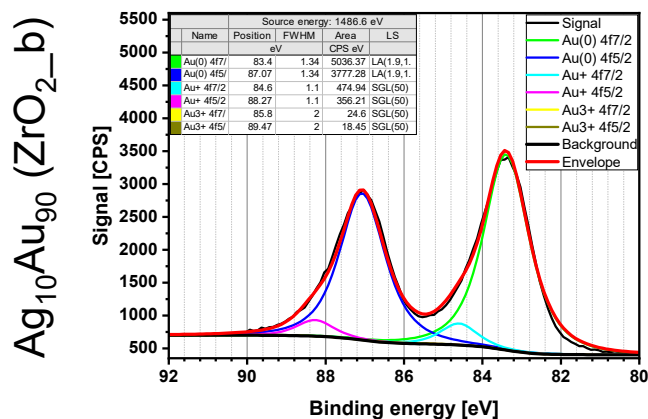
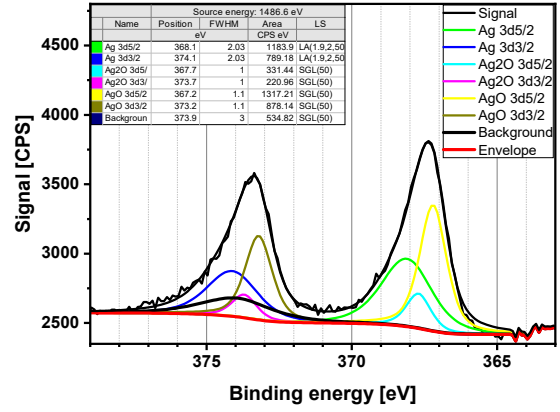
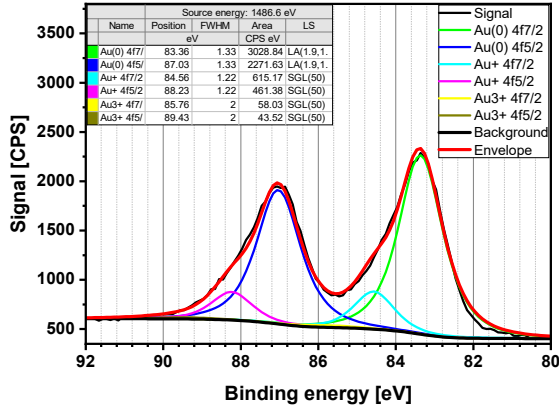


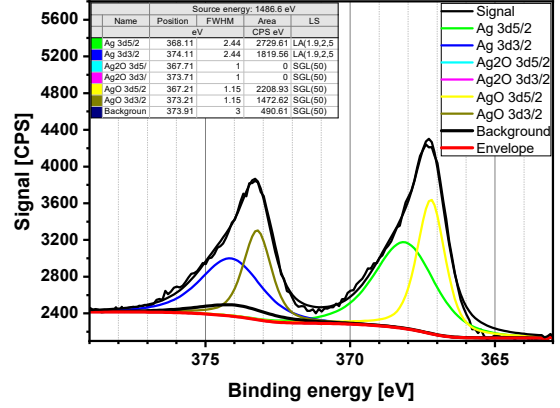
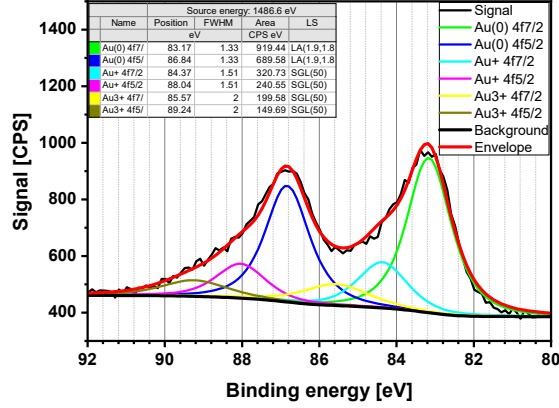
Figure S3 - Calculated surface-area concentrations from the measured mass-concentrations and surface-normalized hydrodynamic size distributions obtained via ADC.



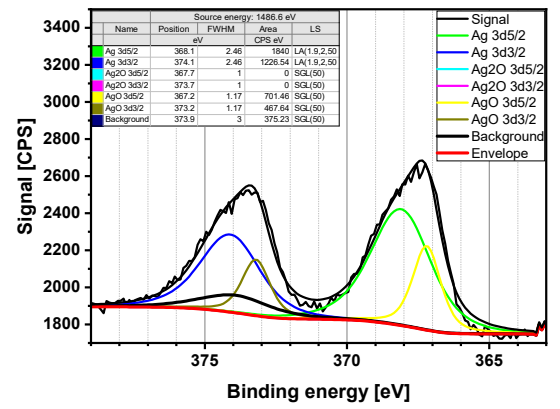
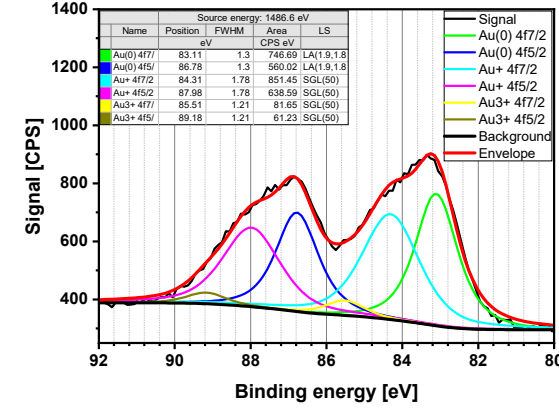
Ag₅₀Au₅₀ (ZrO₂-b)



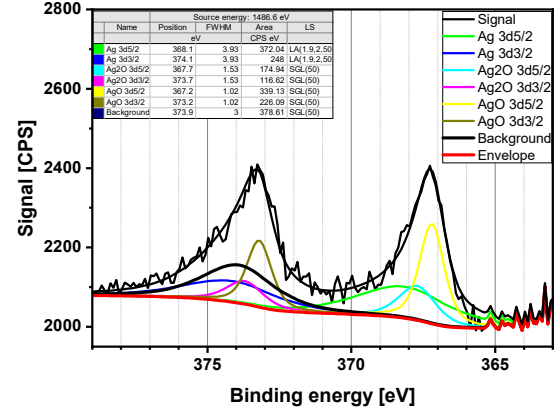
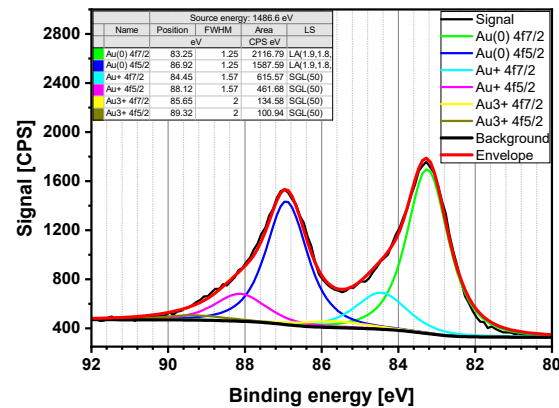
Ag₇₀Au₃₀ (ZrO₂-b)



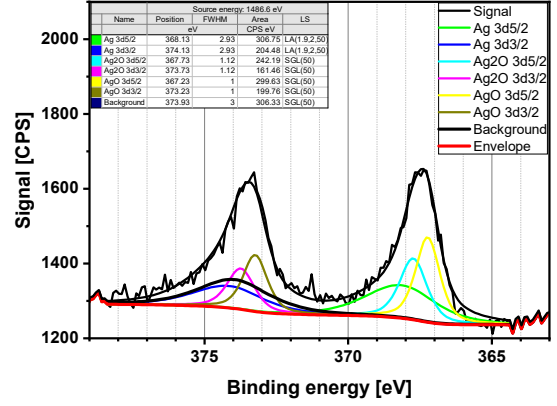
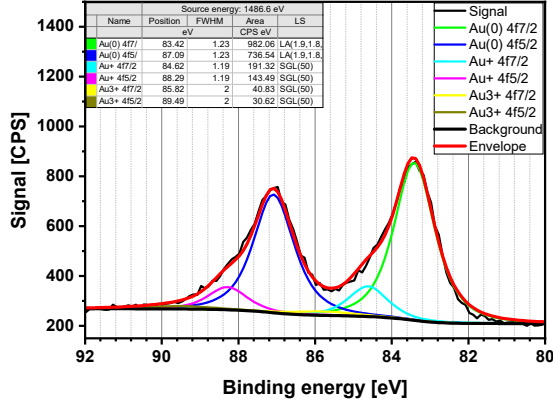
Ag₉₀Au₁₀ (ZrO₂-b)



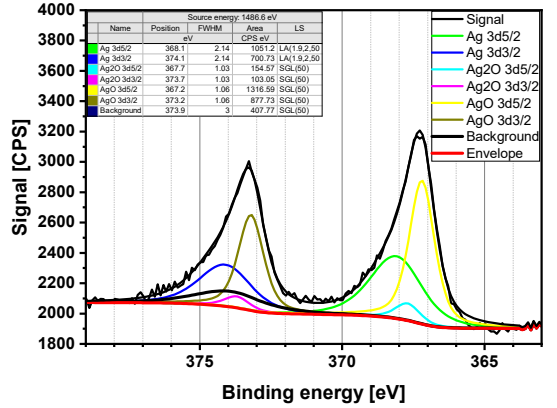
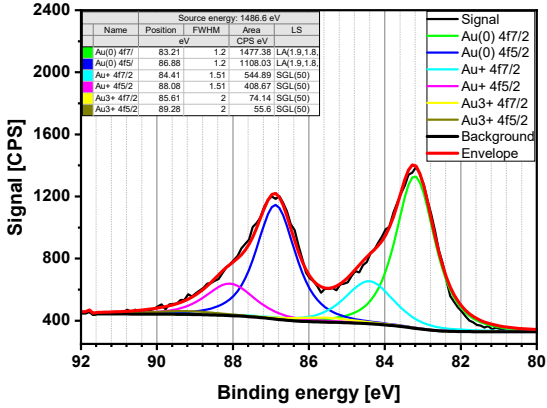
Ag₁₀Au₉₀ (ZrO₂-a)



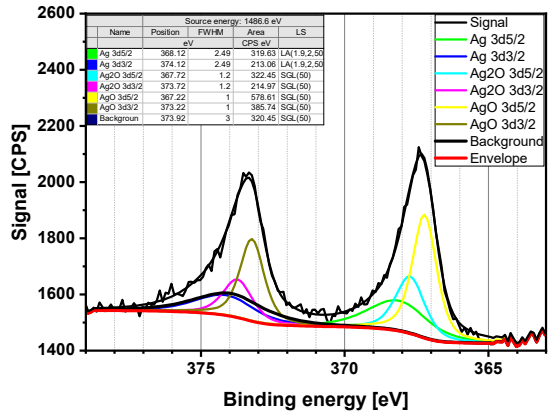
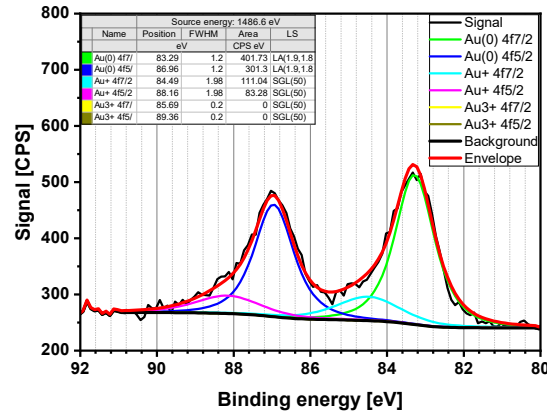
Ag₃₀Au₇₀ (ZrO₂-a)



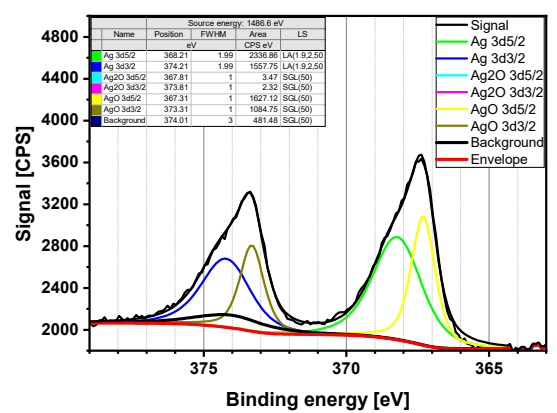
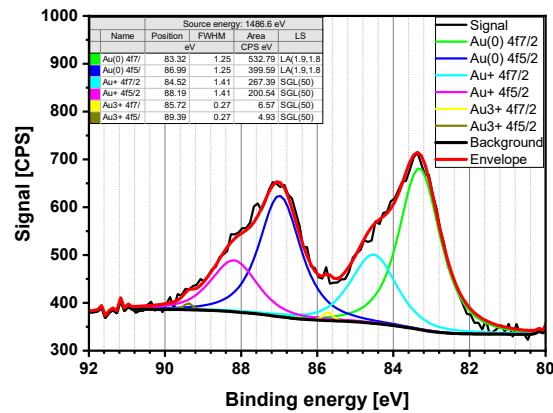
Ag₅₀Au₅₀ (ZrO₂-a)



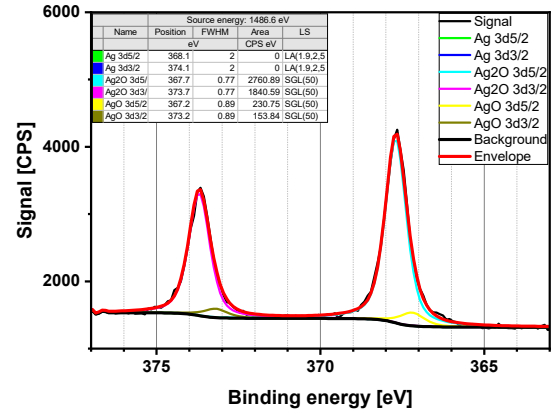
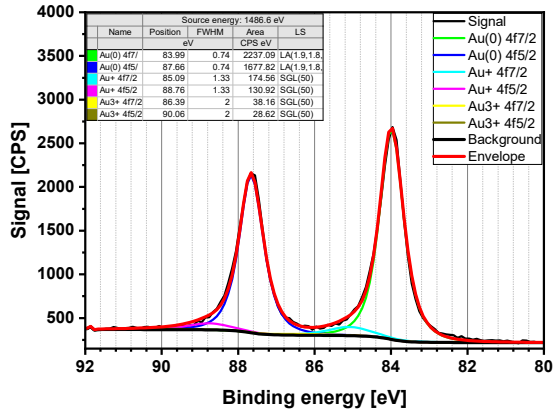
Ag₇₀Au₃₀ (ZrO₂-a)



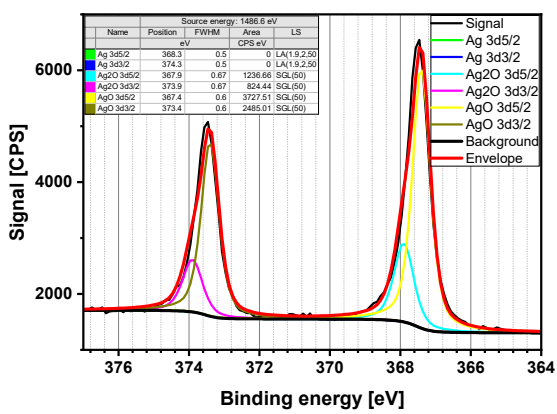
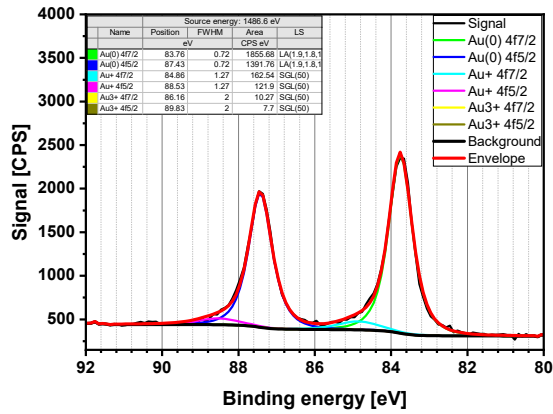
Ag₉₀Au₁₀ (ZrO₂-a)



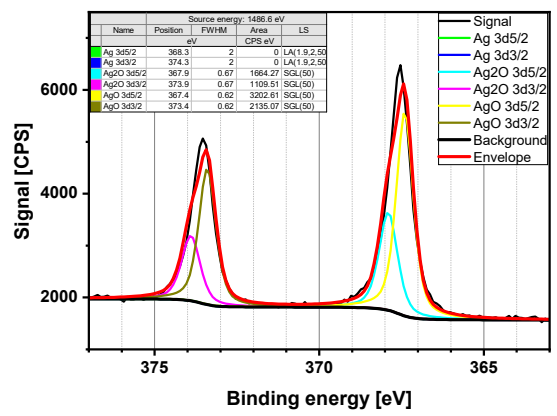
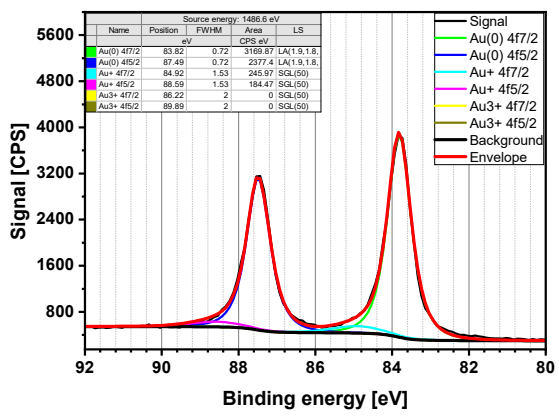
Ag₅₀Au₅₀ (ORR_b)



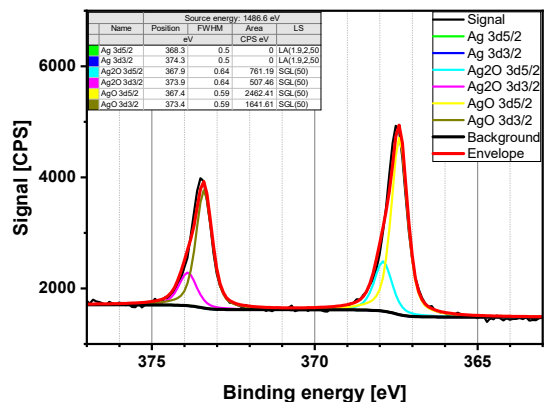
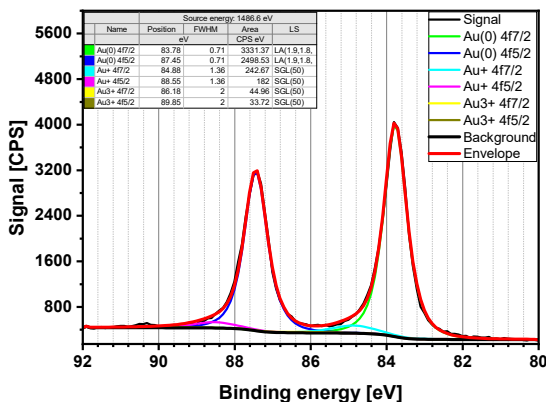
Ag₈₀Au₂₀ (ORR_a)



Ag₅₀Au₅₀ (ORR_a)



Ag₄₀Au₆₀ (ORR_a)



Ag₂₀Au₈₀ (ORR_a)

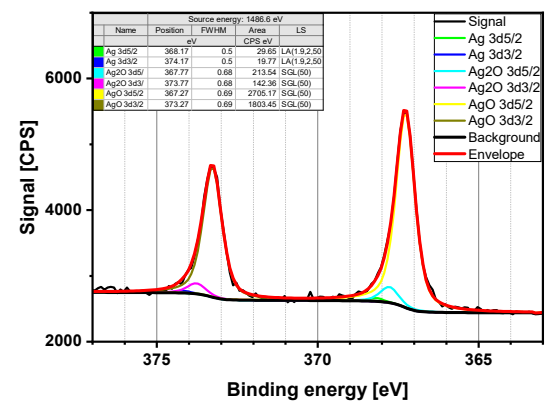
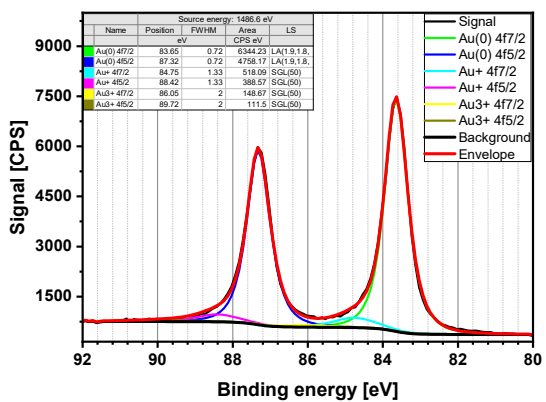


Figure S 4 - Fitted XPS Spectra of the AgAu alloy nanoparticles. From top to bottom, first, come the data of Schade et al. of AgAu NP on ZrO₂ before and after selective oxidation of 5-(hydroxymethyl)furfural (red and blue symbols) has been adapted from Ref. (13). Copyright 2014 CC BY 4.0 <https://creativecommons.org/licenses/by/4.0/legalcode> Wiley-VCH GmbH. The recent measurements performed in this study follow them. We used the following way of naming the samples: The samples analyzed before HMF oxidation are called Ag_xAu_y (ZrO₂_b), while the ones after reaction are Ag_xAu_y (ZrO₂_a). For the recent experiments, we used Ag₅₀Au₅₀ (ORR_b) for the sample measured before ORR, while the ones after ORR are called Ag_xAu_y (ORR_a). The left column shows the fitted signals to gold species, while the right column shows the curves fitted to silver species.

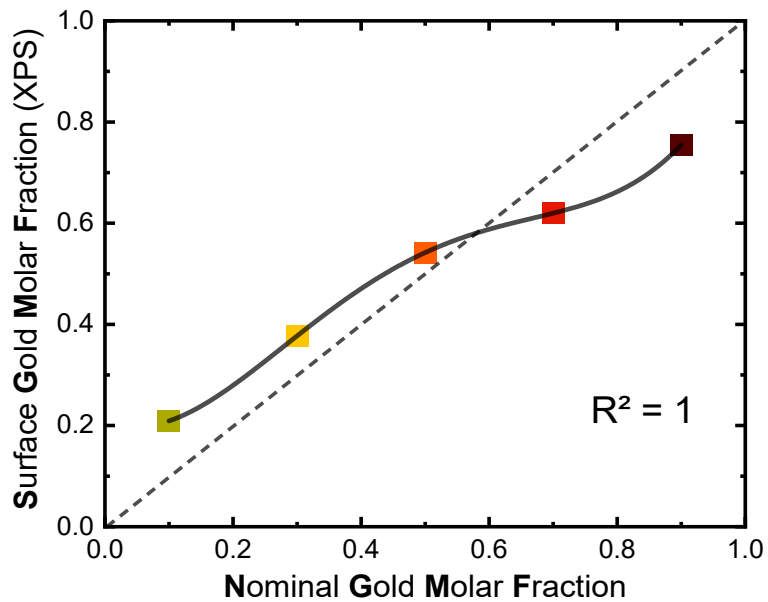


Figure S 5 - Nominal Gold Molar Fraction (x-axis) plotted against the actual Gold Molar Fraction in the surface-near area (y-axis) of silver-gold alloy nanoparticles, analyzed via XPS. The data has been taken from Ref. (1). Copyright 2014 CC BY 4.0 (<https://creativecommons.org/licenses/by/4.0/legalcode>) Wiley-VCH GmbH. We applied a polynomial fit ($R^2=1$) to this data to calculate the expected surface composition from the nominal composition (solid line). The dashed line emphasizes the differences between nominal GMF of each composition and actual surface GMF.

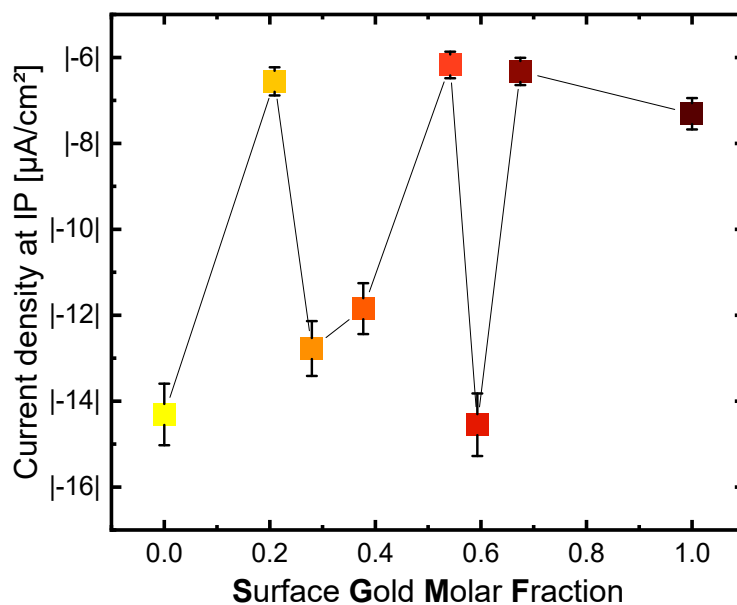


Figure S 6 - Inflection point analysis. Current density in O_2 saturated 0.1 M KOH as a function of the molar surface gold fraction. The data for the surface composition of AgAu NPs has been adapted from Ref. (1). Copyright 2014 CC BY 4.0 (<https://creativecommons.org/licenses/by/4.0/legalcode>) Wiley-VCH GmbH. See **Figure S 5** for the adapted data. The line only guides the eye. The error bars were calculated by repeating the ORR three times.

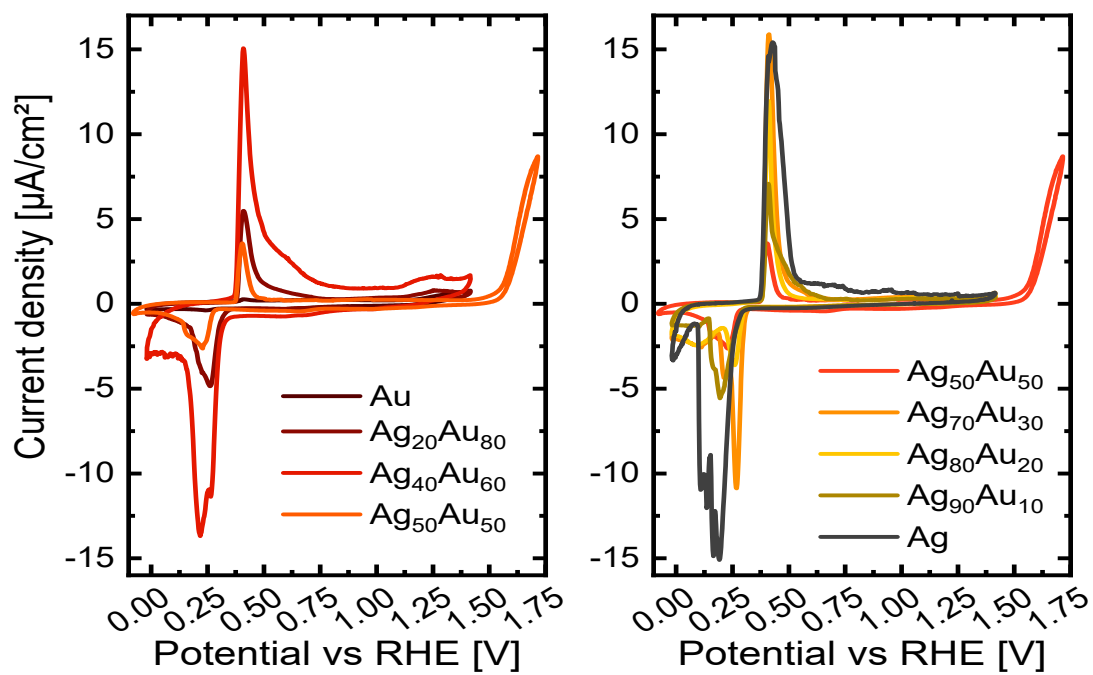


Figure S 7 - CV-diagrams of the pure Au & Ag NPs and their intermediate alloys, measured in N_2 atmosphere with a scan rate of 100 mV/s in 0.1 M HCl. The current density is relative to the applied nanoparticle surface area (see Figure 1 b). Only the 20th cycle is shown to allow easier comparison between the voltammograms.

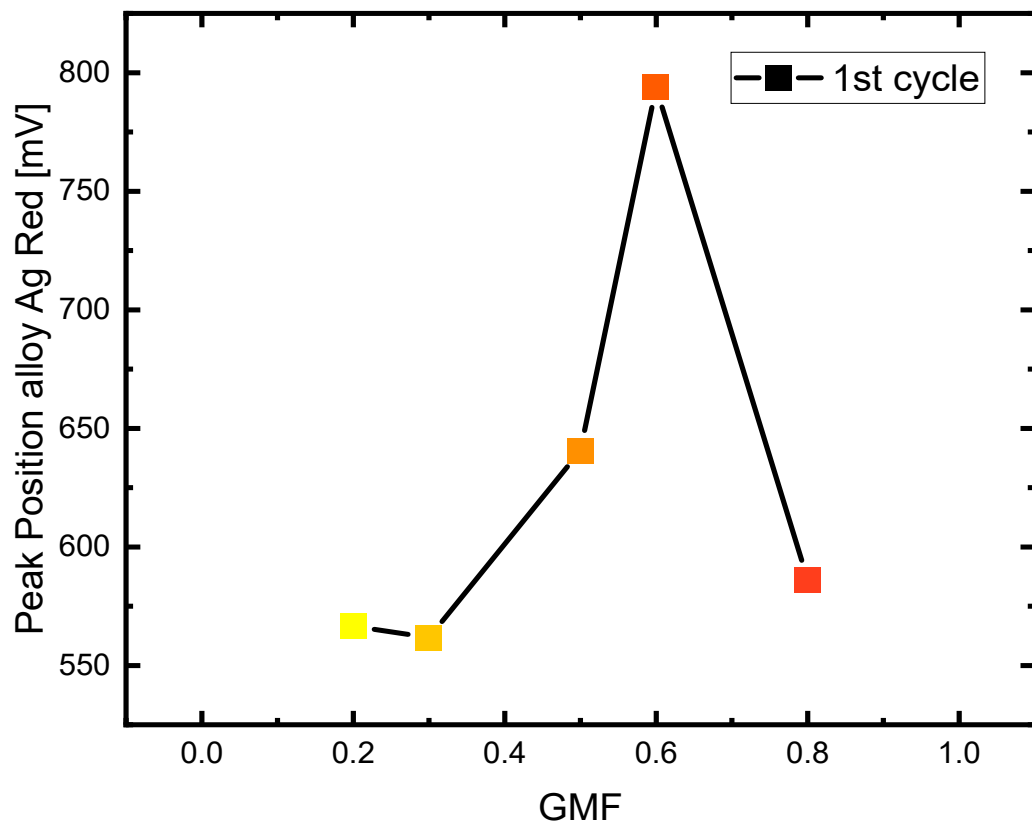


Figure S 8 - Position of the alloyed silver reduction peak as a function of the gold molar fraction in 0.1 M HCl under N₂ atmosphere and a scan rate of 100 mV/s after 1 cycle. The lines guide the eye.

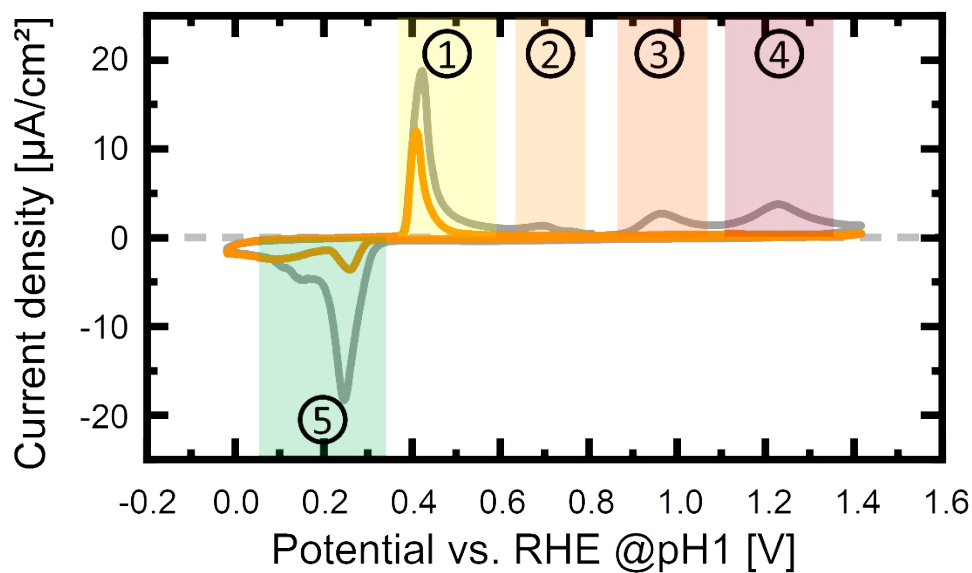


Figure S 9 - Exemplary CVs of the 1st (grey) and 20th (orange) cycle of Ag₈₀Au₂₀ measured in N₂ atmosphere with a scan rate of 100 mV/s in 0.1 M HCl to showcase the regions in which the beforementioned reactions occur: 1) oxidation of silver atoms, 2) oxidation of alloyed silver atoms, 3) oxidation of alloyed gold atoms, 4) oxidation of gold and 5) overlapping reduction reactions of various silver species.

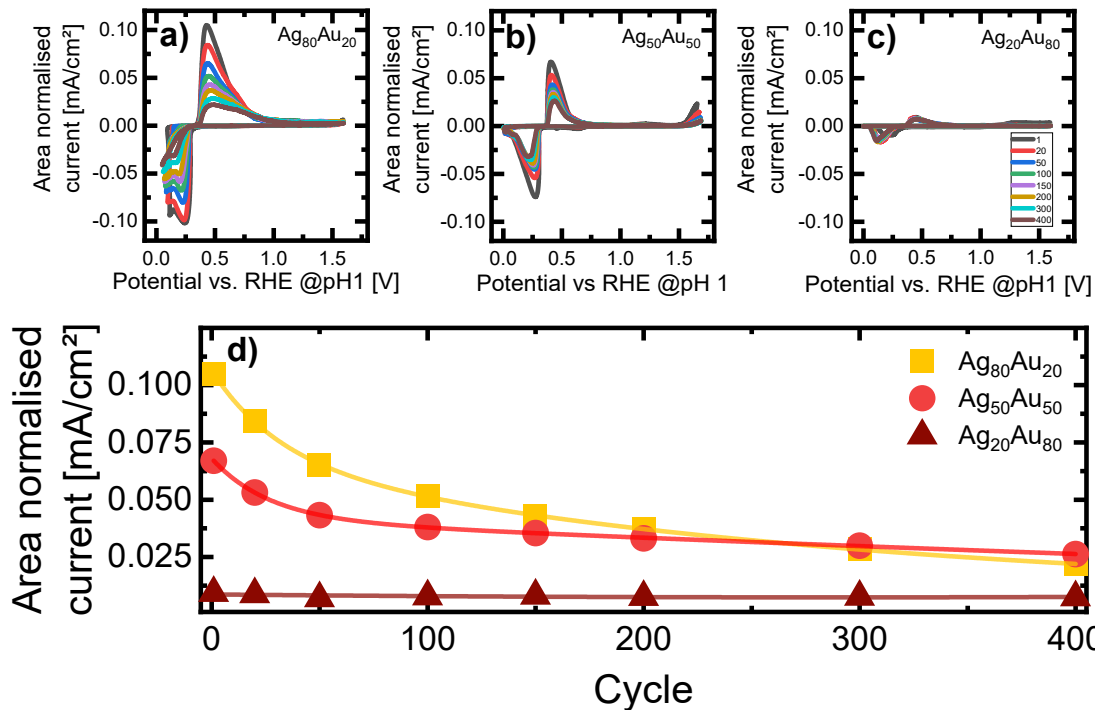


Figure S 10 – Repeated CVs of a) Ag₈₀Au₂₀, b) Ag₅₀Au₅₀ NP & c) Ag₂₀Au₈₀, measured in N₂ atmosphere with a scan rate of 100 mV/s in 0.1 M HCl for up to 400 cycles. The current density is normalized by the nanoparticle surface area. d) shows the reduction in current at the silver oxidation peak in relation to the number of cycles for both compositions. The line is there to guide the eye and empathize the trends.

Table S 2: Charge transferred during silver oxidation and reduction of all tested compositions after 20 cycles.

Composition	Charge transferred during Ag oxidation [μC]	Charge transferred during Ag reduction [μC]
Ag ₂₀ Au ₈₀	119	164
Ag ₄₀ Au ₆₀	141	163
Ag ₅₀ Au ₅₀	64	92
Ag ₇₀ Au ₃₀	132	110
Ag ₈₀ Au ₂₀	110	83
Ag ₉₀ Au ₁₀	129	130
Ag	289	308

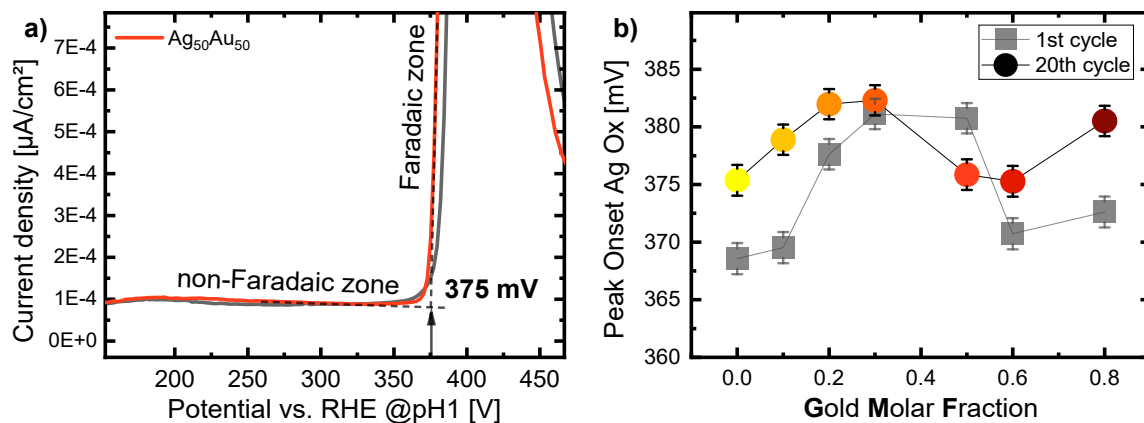


Figure S 11: a) Exemplary representation for the graphical determination of the onset potential and b) Onset of the silver oxidation peak as a function of the gold molar fraction in 0.1 M HCl with a scanning speed of 100 mV/s. The lines guide the eye.

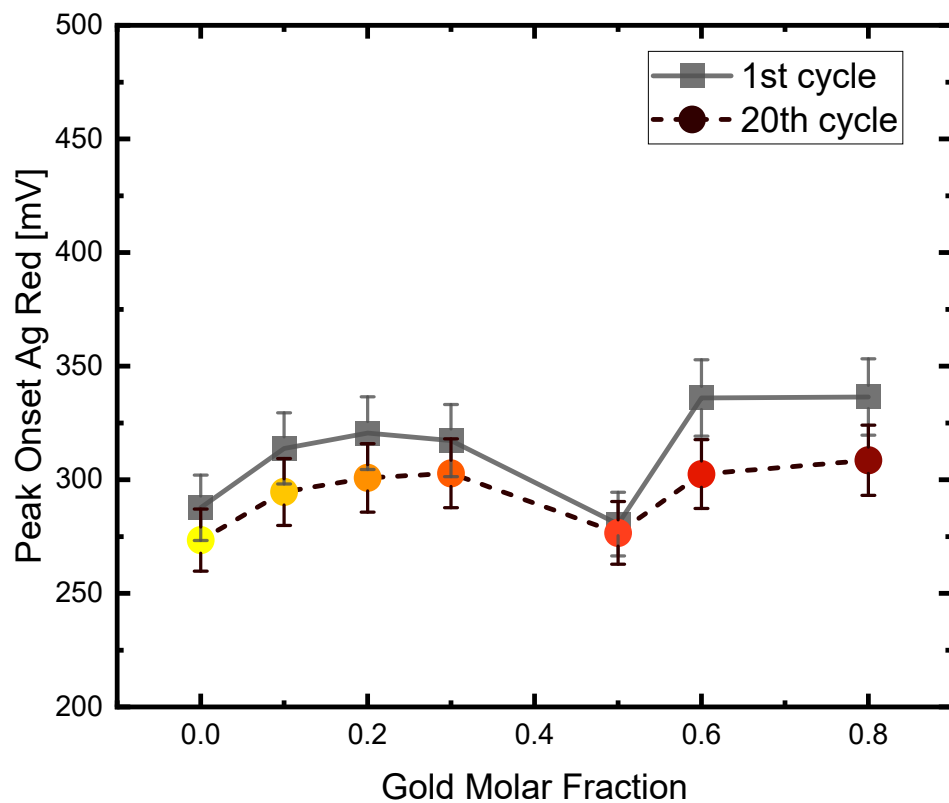


Figure S 12: Onset of the silver reduction peak as a function of the gold molar fraction in 0.1 M HCl with a scanning speed of 100 mV/s. The lines guide the eye.

Table S 3 - Constraints used during fitting of all XPS spectra listed for each element.

Au4f	Au ⁰ (4f 7/2)		Au ⁺ (4f 7/2)	Au ³⁺ (Au 4f 7/2)
	min	max	Au ⁺ =Au ⁰ +X	Au ³⁺ =Au ⁰ +Y
Pos. Constr. / eV	82.4	83.4	X=1.2	Y=2.4
FWHM Constr. / eV	0.7	2.0	=FWHM constr. Au ⁰	=FWHM constr. Au ⁰

Ag3d	Ag ⁰		Ag ⁺	Ag ⁺³⁺
	min	max	Ag ⁺ =Ag ⁰ +X	Au ⁺³⁺ =Au ⁰ +Y
Pos. Constr. / eV	368.1	368.3	X=-0.4	Y=-0.9
FWHM Constr. / eV	1	4	= FWHM constr. Ag ⁰	=FWHM constr. Ag ⁰

References

- 1 O. R. Schade, F. Stein, S. Reichenberger, A. Gaur, E. Saraçı, S. Barcikowski and J.-D. Grunwaldt, Selective Aerobic Oxidation of 5-(Hydroxymethyl)furfural over Heterogeneous Silver-Gold Nanoparticle Catalysts, *Adv. Synth. Catal.*, 2020, **362**, 5681–5696.